Icarus 212 (2011) 779–789

Contents lists available at ScienceDirect

Icarus

journal homepage: www.elsevier.com/locate/icarus

The composition of liquid methane–nitrogen aerosols in Titan's lower atmosphere from Monte Carlo simulations

George Firanescu [a], David Luckhaus [a], Grenfell N. Patey [a], Sushil K. Atreya [b], Ruth Signorell [a,*]

[a] Department of Chemistry, University of British Columbia, 2036 Main Mall, Vancouver, BC, Canada V6T 1Z1
[b] Planetary Science Laboratory, Department of Atmospheric, Oceanic and Space Sciences, University of Michigan, Space Research Building, 2455 Hayward Street, Ann Arbor, MI 48109-2143, USA

ARTICLE INFO

Article history:
Received 28 October 2010
Revised 13 January 2011
Accepted 17 January 2011
Available online 1 February 2011

Keywords:
Titan
Atmospheres, Composition
Clouds

ABSTRACT

Molecular level Monte Carlo simulations have been performed with various model potentials for the CH_4–N_2 vapor–liquid equilibrium at conditions prevalent in the atmosphere of Saturn's moon Titan. With a single potential parameter adjustment to reproduce the vapor–liquid equilibrium at a higher temperature, Monte Carlo simulations are in excellent agreement with available laboratory measurements. The results demonstrate the ability of simple pair potential models to describe phase equilibria with the requisite accuracy for atmospheric modeling, while keeping the number of adjustable parameters at a minimum. This allows for stable extrapolation beyond the range of available laboratory measurements into the supercooled region of the phase diagram, so that Monte Carlo simulations can serve as a reference to validate phenomenological models commonly used in atmospheric modeling. This is most important when the relevant region of the phase diagram lies outside the range of laboratory measurements as in the case of Titan. The present Monte Carlo simulations confirm the validity of phenomenological thermodynamic equations of state specifically designed for application to Titan. The validity extends well into the supercooled region of the phase diagram. The possible range of saturation levels of Titan's troposphere above altitudes of 7 km is found to be completely determined by the remaining uncertainty of the most recent revision of the Cassini-Huygens data, yielding a saturation of 100 ± 6% with respect to CH_4–N_2 condensation up to an altitude of about 20 km.

1. Introduction

Saturn's moon Titan is of considerable interest in the scientific community owing to its Earth-like nitrogen based (>90%) atmosphere, including a hydrological cycle where methane plays the equivalent role of water on our planet (Atreya et al., 2006; Lunine and Atreya, 2008). The analysis of data retrieved by the Cassini-Huygens mission (Fulchignoni et al., 2005; Niemann et al., 2005; Tomasko et al., 2005) suggests the presence of two methane cloud layers separated by a gap (Tokano et al., 2006). Laboratory measurements by Wang et al. (2010a), however, showed that supercooled droplets can be sustained, allowing alternatively for an intermediate supercooled cloud layer instead of a cloud gap. In the upper cloud layer where the cloud particles freeze ($T < 78$ K), nitrogen segregates from methane in the process, leaving almost pure methane particles (Wang et al., 2010a; Tokano et al., 2006). In the two lower layers, however, nitrogen and methane are partially miscible in the liquid droplets. Laboratory aerosol experiments determined a nitrogen content of 30 ± 7% in the liquid droplets ($T \approx 78.5$ K; supercooled liquid droplets) (Wang et al., 2010a). Bulk measurements of Omar et al. (1962) cover a similar temperature range, but they do not extend into the supercooled region and there is also some uncertainty about their accuracy.

In contrast to the *in situ* data, remote observations draw a less clearcut picture so that there is still no consensus among astronomers about the presence of a cloud layer in Titan's troposphere in general. While Ádámkovics et al. (2007) infer widespread equatorial drizzle from near-infrared opacity, Kim et al. (2008) claim to see none, and Penteado et al. (2010) show that Cassini data at the same wavelength can be fit without assuming a condensed layer in the troposphere. De Kok et al. (2010) cite inconsistencies between the presence of a global cloud layer and short-wavelength measurements and propose an increased N_2–CH_4 collision-induced absorption to explain the observed far-infrared opacity. De Kok et al. (2010) in particular point to the *in situ* measurements by the Hyugens probe showing "CH_4 not to be supersaturated at all" (Niemann et al., 2005). The degree of saturation of the troposphere is clearly a crucial parameter in this context, which requires the accurate knowledge of the phase equilibrium. The phenomenological model for the CH_4–N_2 vapor–liquid equilibrium (VLE) used to analyze the Huygens data actually indicated a small but significant

* Corresponding author. Fax: +1 604 822 2847.
E-mail address: signorell@chem.ubc.ca (R. Signorell).

0019-1035/$ - see front matter © 2011 Elsevier Inc. All rights reserved.
doi:10.1016/j.icarus.2011.01.021

undersaturation at altitudes between 7 and 18 km (CH_4 saturation levels of 80–90%, *vide infra*). The accuracy of those models thus becomes a central issue for the discussion. Furthermore, the composition of the liquid droplets is obviously important for cloud modeling of Titan's atmosphere (Barth and Toon, 2006; Graves et al., 2008; Barth and Rafkin, 2010, 2007), but the Cassini-Huygens mission was not equipped for such measurements. Even in laboratory experiments the composition of the liquid aerosol droplets is difficult to determine at such low temperatures – to our knowledge Wang et al. (2010a) report the only direct aerosol measurements available in the literature.

It is thus clear that modeling the CH_4–N_2 VLE is crucial for the understanding of Titan's atmosphere, which immediately raises the issue of the accuracy of commonly used approaches. Current cloud models rely on empirical thermodynamic models to extrapolate the CH_4–N_2 phase equilibrium to the conditions prevalent on Titan. Among the more widely used approaches are those devised by Kouvaris and Flasar (1991) and by Thompson et al. (1992). The temperature and pressure range of interest, however, lies partly outside the range of reliable experimental information on which those models were built so that their accuracy must be considered uncertain. The model of Kouvaris and Flasar, e.g. is based on experimental data on the methane–nitrogen mixture recorded above the triple point of methane (90.68 K). Below that, vapor pressure curves of mixtures down to their respective triple points were taken from the work of Omar et al. (1962), but the accuracy of these data has been questioned (Thompson et al., 1992). Moreover, some of the measurements for bulk mixtures have relatively large uncertainties of up to 7%, and even a few inconsistencies have been noted (Kouvaris and Flasar, 1991).

Both empirical thermodynamic models contain a large number ($\sim$25) of adjustable parameters giving them the flexibility to fit a broad range of experimental data. This same flexibility, however, diminishes the reliability of any extrapolation beyond the range of experimental data, which makes an independent validation all the more important. In this contribution we report on Monte Carlo (MC) simulations of the phase equilibrium of CH_4–N_2 mixtures in the temperature and pressure range prevalent in Titan's atmosphere up to altitudes of 18.6 km. Since the simulations are based on a molecular representation of the mixture they provide a completely independent description of the phase equilibrium that can be compared with the empirical thermodynamic models. The minimal number of adjustable parameters of the underlying pair potential models (only a single one to describe the mixing properties) allows for a particularly robust extrapolation of the MC simulations beyond the range of experimental data, so that they provide a reliable reference for assessing the accuracy of empirical thermodynamic models for predictions in that range. Prior to that it is of course necessary to demonstrate that such simple potential models can describe available experimental data with the requisite accuracy. In our MC simulations we test simplified pair potentials from various sources to describe intermolecular interactions. It turns out, that all potentials that properly reproduce the vapor pressure and densities of the pure liquids up to about 40 K above the respective triple points, yield similar results for the mixture. A minor adjustment of the cross-interaction (i.e. between unlike molecules) to reproduce a single bulk measurement at a higher temperature brings these MC simulations into almost perfect agreement, both with each other and with observed experimental data. The remaining small deviations provide estimates for the uncertainties of predictions of the vapor–liquid equilibrium of CH_4–N_2 binary aerosols in Titan's atmosphere from the surface up to an altitude of 18.6 km, which lies in the supercooled region. In this region the phenomenological models of Kouvaris and Flasar (1991) and of Thompson et al. (1992) show small but systematic deviations from the MC results. We discuss the results in relation to the gas phase composition determined by Cassini-Huygens, including the very recently revised analysis by Niemann et al. (in press), and the possible role of other atmospheric trace components in determining the aerosol droplet composition.

2. Modeling

In the present work we compare molecular level Monte Carlo simulations with results obtained from three different empirical equations of state (EOS). The molecular simulations are based on model interaction potentials parameterized to reproduce certain bulk data of pure substances (liquid densities, vapor pressures) or *ab initio* results for two-body interactions. As *ab initio* calculations show that three-body interactions are negligibly small for pure methane and nitrogen (a few percent of two-body interactions; this work and Szczesniak et al. (1990)) all model potential functions consist of pairwise additive terms.

2.1. Monte Carlo simulations

In the present work we simulate the vapor–liquid equilibrium (VLE) for binary CH_4–N_2 mixtures in the grand canonical (GCMC) and in the Gibbs ensemble (GEMC). The GCMC simulations were used to guide the test calculations of the different potential models independently of empirical EOS data. At the same time they served as a consistency check for the GEMC calculations, in particular at very asymmetric phase compositions and low temperatures, and to address concerns regarding the possible number-dependence of Gibbs-ensemble simulations (Valleau, 1998). Both GCMC and GEMC calculations employed the Metropolis algorithm for standard Boltzmann sampling without any additional bias as described in Allen and Tildesley (1988) and Frenkel and Smit (2001).

The GCMC simulations were performed in a cubic cell with an edge length of $L = 30$ Å, using periodic boundary conditions and a standard cut-off at $L/2$ for all molecular interactions. Standard isotropic long range corrections (Allen and Tildesley, 1988; Frenkel and Smit, 2001) were applied to energy and pressure at each step. The simulation box typically contained $N = 400$–500 molecules in the liquid phase and up to about 40 molecules in the gas phase. One GCMC run consisted of 8×10^8 steps, with data sampled every 10 steps. In each step a molecular species is randomly selected followed by one of three operations applied with equal probability to a randomly selected molecule of that type: (a) insertion, (b) deletion, (c) translation/rotation. Liquid phase properties are typically averaged over 20 runs for pure substances and 80 runs for the mixture.

VLE points were computed for given pressure and temperature (P,T) using the following iterative procedure: The iteration starts with the chemical potentials derived from a guess for the composition of the vapor phase at (P,T) assuming ideal gas behavior. In a second step the approximate zero of the pressure as a function of the chemical potentials is determined in the liquid phase. The resulting chemical potentials are then used as a starting point to match the pressure of the real vapor phase (calculated as a function of chemical potential) with the given pressure P. The second and the third step are repeated until the chemical potentials of the two phases match. The statistical uncertainty of the sampling is insignificant compared with the uncertainty arising from any mismatch between liquid and gas pressure. For the current system a difference of 0.5–1.0 bar, depending on conditions, is sufficient to achieve an accuracy of 1% in vapor pressure, equivalent to that of measurements by the Huygens probe in Titan's atmosphere. At constant (P,T), compositions in terms of mole fractions are accurate within 10^{-3} (i.e. 2–3 significant digits).

The final MC predictions for the aerosol phase equilibrium in Titan's atmosphere were obtained from isobaric GEMC simulations

with similar parameters as in the GCMC simulations, but $N = 100$–200 molecules in the vapor compartment. The larger number of gas phase molecules was chosen to improve the statistics for extremely asymmetric mixtures (mole fractions $x_{CH_4} \ll 0.1$). In addition to the basic operations to sample the isobaric Gibbs ensemble (volume change, particle exchange between compartments, translation/rotation) we introduced a particle identity swap, which corresponds to a particle exchange that keeps coordinates unchanged (Panagiotopoulos, 1989; Martin and Siepmann, 1997). This additional operation improves the sampling of compositions as it has a much higher acceptance rate than random insertion, especially for the higher liquid densities at low temperatures. The probabilities of applying any of the four types of operations were 2×10^{-3}, 0.95, 0.04, and 0.01, respectively. Final results were averaged over 2–5 $\times 10^{10}$ samples. Standard deviations over block averages of 8×10^7 samples each indicate that mole fractions are accurate to three significant digits which was checked in a few cases with averages over up to 1.5×10^{11} samples. We checked that our final results are free of finite size effects by varying both N (up to 1800 molecules) and the average overall ensemble composition (which determines the average number of particles per compartment).

2.2. Potential models

Monte Carlo (MC) simulations require a potential model to describe the intermolecular interactions. To determine the sensitivity of our composition predictions for liquid CH_4–N_2–aerosol particles to the type of intermolecular potential and to its parametrization, we carried out simulations using several models. The VLE of pure methane and nitrogen has been modeled extensively resulting in several potential models for each substance (Chao et al., 2009; Lotfi, 1993; Murthy et al., 1980; Potoff and Siepmann, 2001; Shadman et al., 2009; Vrabec et al., 2001), which leaves the model for the cross-interaction between unlike molecules to be determined. In contrast to the pure substances, few efforts have been made to model the CH_4–N_2 mixture at a microscopic level (Carrero-Mantilla and Llano-Restrepo, 2003; Shadman et al., 2009), and none in the temperature range relevant to Titan. We chose the potential combinations from Carrero-Mantilla and Llano-Restrepo (2003) and Shadman et al. (2009) as a starting point and made refinements as necessary.

The models referred to in the present work describe the pairwise interaction with a combination of Lennard–Jones (LJ) potential functions U_{LJ}, and electric multipole interactions with varying parameterizations:

$$U_{LJ} = 4\epsilon_{ab}\left[\left(\frac{\sigma_{ab}}{r}\right)^{12} - \left(\frac{\sigma_{ab}}{r}\right)^{6}\right] \tag{1}$$

ϵ_{ab} is the well depth, σ_{ab} the effective collision radius and r the distance between two sites. The indices a and b refer to the type of interaction site on different molecules. Here we use the modified Lorentz–Berthelot rules to parameterize the interaction between unlike sites on different molecules:

$$\epsilon_{ab} = \delta_\epsilon\sqrt{\epsilon_a\epsilon_b} \tag{2}$$

$$\sigma_{ab} = \delta_\sigma(\sigma_a + \sigma_b)/2 \tag{3}$$

δ_ϵ and δ_σ are adjustable scaling parameters. Except where otherwise noted we set $\delta_\sigma = 1$.

Multipole interactions can be either modeled explicitly or included in an effective way in the LJ potential. We tested both variants for comparison. The most significant multipole interaction in the CH_4–N_2 system is the quadrupole–quadrupole interaction between nitrogen molecules. For linear molecules it can be expressed as:

Table 1
Parameters for the model potentials used in the MC simulation (notation as in Section 2.2). Site types: nLJ – n Lennard–Jones sites; Q – point quadrupole.

	M1-N_2 [a]	M2-N_2 [e]	S-N_2 [b]	F-N_2 [e]
N_2				
Sites	2LJQ	2LJQ	1LJ	1LJ
σ (Å)	3.318	3.298	3.5613	3.5989
ϵ (K)	36.4	36.4	95.99	99.72
r_{NN} (Å)	1.098	1.098		
Q (eÅ^2)	0.244	0.244		
	L-CH_4 [c]	C-CH_4 [d]	S-CH_4 [b]	F-CH_4 [e]
CH_4				
Sites	1LJ	4LJ	1LJ	1LJ
σ (Å)	3.7275	2.67	3.732	3.7206
ϵ (K)	148.99	27.17	151.15	149.74
r_{CH} (Å)		1.085		

[a] Murthy et al. (1980).
[b] Shadman et al. (2009).
[c] Vrabec and Fischer (1996).
[d] Chao et al. (2009).
[e] This work.

$$U_{QQ} = \frac{3Q_iQ_j\Omega_{ij}}{16\pi\varepsilon_0 r_{ij}^5} \tag{4}$$

where

$$\Omega_{ij} = 1 - 5\cos^2\theta_i - 5\cos^2\theta_j - 15\cos^2\theta_i\cos^2\theta_j + 2(\boldsymbol{e_i}\cdot\boldsymbol{e_j} - 5\cos\theta_i\cos\theta_j)^2 \tag{5}$$

$$\cos\theta_i = \frac{\boldsymbol{e_i}\cdot\boldsymbol{r_{ij}}}{r_{ij}} \tag{6}$$

Q_i is the quadrupole moment of molecule i, ε_0 is the vacuum electrical permittivity, $\boldsymbol{r_{ij}}$ is the vector pointing from the center of mass of molecule i to that of molecule j and $\boldsymbol{e_i}$ are unit vectors along the molecular axes. A complete list of all potential parameters used in this paper and their short hand notation used throughout the rest of the paper is given in Table 1.

Our first potential choices follow the work of Carrero-Mantilla and Llano-Restrepo (2003) who computed the vapor–liquid equilibrium curves of CH_4–N_2 between 130 and 170 K. Using the Lorentz–Berthelot combining rules (Eqs. (2) and (3)) with δ_ϵ, $\delta_\sigma = 1$ they obtained good agreement with the experimental results of Kidnay et al. (1975).

2.2.1. M1-N_2 potential

N_2 was modeled by an empirical potential developed by Murthy et al. (1980). Their model is comprised of two LJ sites placed on the nitrogen atoms and a point quadrupole placed at the molecular center of mass. Parameters were fitted to the lattice constant and sublimation energy of the α-N_2 solid phase and to the second virial coefficient of the gas. The model was validated for VLE calculations by Carrero-Mantilla and Llano-Restrepo (2003) reproducing the density of the liquid between 75 and 120 K within 2% (estimated from Fig. 1 of their article). Calculations in Section 3.1 reveal a systematic underestimation of the vapor pressure by 4%.

2.2.2. M2-N_2 potential

The pure N_2 VLE curve of the M1-N_2 potential has exactly the same shape as the experimental one (Lemmon et al., 2010), but is slightly shifted to lower pressures. Decreasing σ by 0.02 Å yields virtually exact agreement (deviations <0.1%), far below the uncertainty in pressure measurements on Titan (1%).

2.2.3. L-CH_4 potential

CH_4 was described by the single LJ site potential of Lotfi (1993) fitted simultaneously to the experimental vapor pressure and

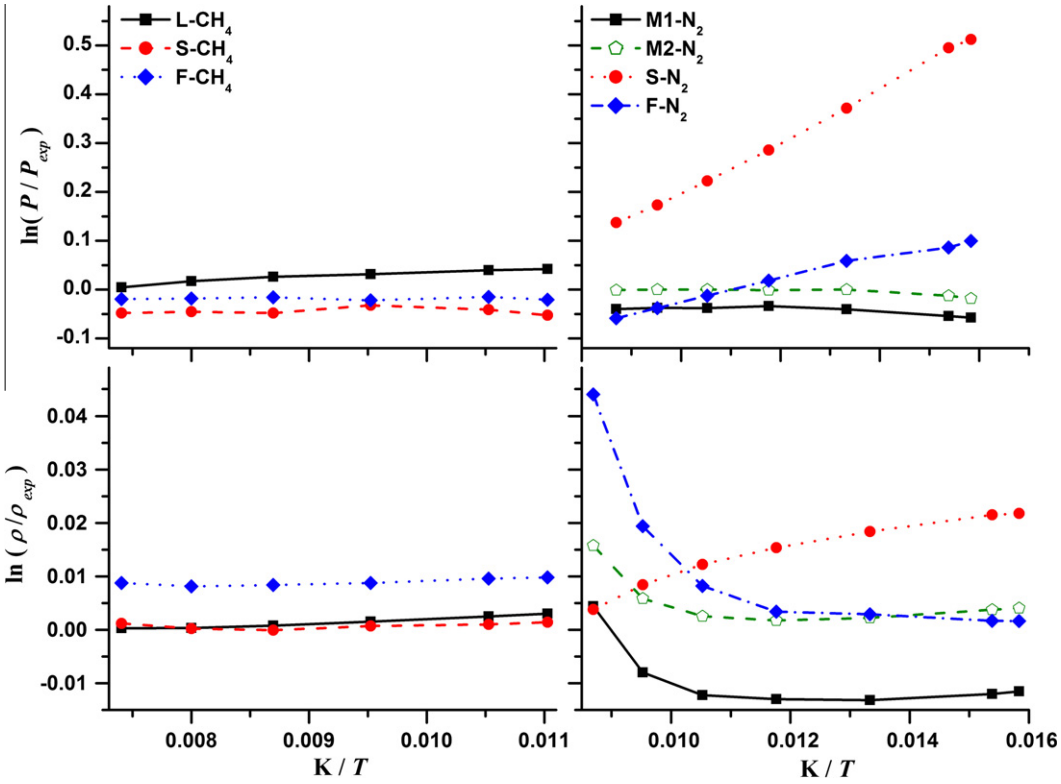

Fig. 1. Deviations between calculated and experimental vapor pressure (upper panels) and liquid density curves (lower panels) of pure methane (lhs) and pure nitrogen (rhs). The calculated curves were obtained from GCMC simulations with the potential models defined in Section 2.2.

density at 140.63 K. The model was validated against a very accurate CH_4 equation of state (Setzmann and Wagner, 1991) that reproduces the experimental density within 0.03% for pressures below 12 MPa and temperatures from 90 K to 350 K and within 0.15% above 350 K. We computed the VLE curve of this model (see Section 3.1) between 95 K and 135 K. The pressure deviations obtained increase from −1% to 4%, the latter value being consistent with Lofti's error estimate.

2.2.4. S-CH_4 and S-N_2 potentials

Our second choice are the *ab initio* potentials of Shadman et al. (2009) derived for the CH_4–N_2 interaction. Following the work of Schindler et al. (1993), they computed an improved *ab initio* potential energy surface (PES) of the hetero-dimer at the MP2 level of theory with cc-pVXZ and aug-cc-pVXZ (X = D, T, Q) basis sets for 12 orientations using rigid monomers. The PES was extrapolated to the complete basis set limit and fitted via least squares to single LJ site potentials located at the molecular center of mass for both N_2 and CH_4.

2.2.5. F-CH_4 and F-N_2 potentials

We fitted single LJ site potentials simultaneously to the experimental *P*–*T* saturation curves and densities of pure methane between 91 K and 140.5 K, and of pure nitrogen in the range of 70–120 K (Lemmon et al., 2010). The least-squares fit employed the LJ equation of state derived by Johnson et al. (1993), which reproduces the VLE of the LJ fluid to within better than 1% (see Section 2.3.1). The densities were included in the fit with a weight factor of 1/3, which was chosen so as to achieve an even distribution of the relative error in density and vapor pressure over the temperature range of interest. We note that the vapor pressure alone does not provide a sufficient constraint for the LJ parameters, which can lead to errors in the density of up to 34%.

2.2.6. C-CH_4 potential

Chao et al. (2009) fitted an anisotropic potential model for CH_4 to an *ab initio* PES of the dimer obtained from high level theory calculations up to MP2/aug-cc-pVXZ (X = D, T, Q) for 12 conformers over a wide range of C–C distances (3–9 Å) to a total of 732 configuration points, and extrapolating to the complete basis set limit. The resulting 4 site LJ potential with interaction sites placed on the H atoms (r_{CH} = 1.085 Å) reproduces the radial distribution function of liquid CH_4 at 150 K and the self-diffusion coefficient in the range of 112–207 K.

2.2.7. Cross-interaction

Potential models for the mixture are defined in terms of the pure substance potential functions and the scaling δ_ϵ of the cross-interaction of unlike molecules (Eq. (2)), e.g. F-CH_4/M2-N_2[δ_ϵ]. If not explicitly stated otherwise the size parameter scaling δ_σ (Eq. (3)) was set to 1.0 throughout our calculations. δ_ϵ was manually adjusted to reproduce experimental gas and liquid phase compositions of the CH_4–N_2 mixture. As there is some uncertainty regarding the accuracy of the low temperature data of Omar et al. (1962) (Kouvaris and Flasar, 1991; Thompson et al., 1992), we decided to use data from Kidnay et al. (1975) instead. These data are only available for higher pressures and temperatures, but have been checked for thermodynamic consistency (Thompson et al., 1992). We selected the experimental equilibrium composition for the four lowest (*P*,*T*)-values available from Kidnay et al. (1975): 1.965 and 4.332 bar at 112 K, and 4.155 and 6.594 bar at 130 K. For δ_ϵ = 1 the relative error of simulated CH_4 mole fractions reaches up to 11%, invariably underestimating the methane content of both phases. Damping the cross interaction by a few percent (see Table 3) typically reduces this error by a factor of 2–3, except for the S-CH_4/S-N_2[δ_ϵ] combination, where only a minor improvement was obtained. With a residual error arising in the third significant digit

of x_{CH_4}, the F-CH_4/M2-N_2[δ_ϵ] potential affords the best agreement for the lowest (P,T)-value (1.965 bar at 112 K), which still lies about 20–30 K above typical values on Titan.

2.3. Equations of state

We compare the molecular MC simulations with the results predicted from three different equations of state (EOS): The van der Waals one-fluid model for LJ fluids (LJ–vdW1) (Johnson et al., 1993), the model of Thompson et al. (1992), and the model of Kouvaris and Flasar (1991). The latter two were designed specifically for application to Titan.

2.3.1. The Lennard–Jones van der Waals one-fluid model

As shown in Section 3.1, the VLE curves of CH_4 and N_2 follow rather accurately those of a LJ fluid, i.e. up to the temperature and length scales defined by the respective LJ parameters (Eq. (1)), they are described by the same EOS. In this case the van der Waals one-fluid theory provides a simple extension to mixtures by introducing composition dependent LJ parameters. Johnson et al. (1993) have proposed a compact and accurate analytical representation of the LJ EOS. All quantities of interest are derived from the excess Helmholtz free energy:

$$A_r^* = A^* - A_{ideal}^* = \sum_{i=1}^{8} \frac{a_i \rho^{*i}}{i} + \sum_{i=1}^{6} b_i G_i \tag{7}$$

where * denotes scaled quantities ($A^* = A/N\epsilon$, $T^* = Tk_B/\epsilon$, $\rho^* = \rho\sigma^3$, etc.). The expansion coefficients $a_i(T^*)$, $b_i(T^*)$, and $G_i(\rho^*)$ are defined in terms of 33 independent parameters (see Johnson et al., 1993), which were fitted to Molecular Dynamics simulations over a broad range of temperatures ($0.7 \leqslant T^* \leqslant 6.0$) and densities ($0.005 \leqslant \rho^* \leqslant 1.25$). Note that the fit did not include data points in the metastable range below the triple point of the LJ fluid ($T^*_{triple} \approx 0.69$). The LJ–vdW1 model for the mixture is obtained by replacing the LJ parameters in the scaling expressions with weighted averages according to the following mixing rules (Johnson et al., 1993; McDonald, 1973) with a = CH_4 and b = N_2:

$$\sigma_x^3 = \sum_a \sum_b x_a x_b \sigma_{ab}^3 \tag{8}$$

$$\epsilon_x = \frac{1}{\sigma_x^3} \sum_a \sum_b x_a x_b \epsilon_{ab} \sigma_{ab}^3 \tag{9}$$

In analogy to the potential models we use, the cross-interaction scaling (Eq. (2)) is indicated in brackets, i.e. LJ–vdW1[δ_ϵ].

2.3.2. The Kouvaris model

Kouvaris and Flasar (1991) derived an isobaric phase coexistence equation for the CH_4–N_2 binary mixture between 75 K and 120 K from the Gibbs–Duhem equation by integrating (Eq. (10)):

$$\frac{dy_1}{dT} = \frac{y_1(1-y_1)}{y_1 - x_1}\Omega - y_1(1-y_1)\frac{df_{12}}{dT} \tag{10}$$

with Ω and f_{12} approximated at the low pressures of interest here through

$$\Omega = \frac{\Delta H^L - x_1 L_1 - x_2 L_2}{RT^2} \tag{11}$$

$$f_{12} = \frac{(2B_{12} - B_{11} - B_{22})P}{RT}(1 - 2y_1) \tag{12}$$

R is the molar gas constant, x_i and y_i are liquid and gas phase mole fractions, respectively, and the indices indicate CH_4 (1) and N_2 (2). The heat of mixing of the liquid ΔH^L and the equilibrium heats of vaporization L_i were obtained from experimental data (McClure et al., 1976; Angus et al., 1978, 1979), while the virial coefficients B_{ij} were determined from Bender's EOS (Bender, 1975).

Expressions for $x_1(T,P = const)$ isobars with pressures ranging from 200 to 4000 mbar were derived in three steps: From a self-consistent set of experimental isotherms between 90 K and 125 K (Cheung and Wang, 1964; Sprow and Prausnitz, 1966; Parrish and Hiza, 1974; Cines et al., 1953; McClure et al., 1976) $P(T,x_1 = const)$ isopleths were interpolated for ten x_1 values and combined with corresponding measurements of Omar et al. (1962) in the 60–90 K range. A quadratic from for $\ln(P(T))$ served to extrapolate into the supercooled region. Finally $x_1(T,P)$ was obtained by cubic spline interpolation of the set of $P(T;\ x_1 = const)$ isopleths at constant pressure. As Kouvaris et al. did not specify the type of interpolation in the first step, we used a third-order polynomial. The experimental data below 90 K had to be read from Fig. 14 of Omar et al. (1962) as no numerical values were given. The y_1 values thus determined typically deviate less than 0.003 from those calculated in the experimental works used in the fit. Large differences of up to 0.022 in y_1 were obtained relative to the data of Cheung and Wang (1964), which were deemed unreliable. According to Kouvaris and Flasar (1991) an estimated error in x_1 of 0.01 translates into an error of 0.002 in y_1 for CH_4-rich liquids ($0.8 \leqslant x_1 \leqslant 1.0$), which becomes much smaller for $x_1 < 0.8$.

2.3.3. The Thompson model

Thompson et al. (1992) derived an empirical equation of state for the CH_4–N_2 system for applications to Titan, strongly constraining the model's temperature dependence by utilizing both VLE and heat of mixing measurements in the fitting procedure. The core of the model is a generalized Raoults's law expression for non-ideal systems:

$$\phi_i(T,P) y_i P = \gamma_i(T,P) x_i \phi_i(T, P_i^{sat}) P_i^{sat} \tag{13}$$

The pressure P and temperature T define the equilibrium state. P_i^{sat} is the vapor pressure of pure component i. The fugacity coefficients ϕ_i are derived from a virial expansion up to third order. The second virial coefficients were obtained by the method of Hayden and O'Connell (1975) and the third-order coefficients by the method of Orbey and Vera (1983) in conjunction with the Prausnitz (1969) mixing rules. These methods require the triple point and critical point data as well as molecular acentric factors and gyration radii as input (Thompson et al., 1992). The activity coefficients γ_i were obtained from the excess Gibbs energy G^E through the Gibbs–Duhem relation. The functional form of G^E was simultaneously fitted to experimental VLE (McClure et al., 1976; Parrish and Hiza, 1974; Kidnay et al., 1975; Stryjek et al., 1974) and excess enthalpy data (McClure et al., 1976). The fit data ranging from 114 K down to the triple point of methane were selected according to thermodynamic consistency tests. The pure component vapor pressures P_i^{sat} were obtained from the equations of Iglesias-Silva et al. (1987) which are expected to extrapolate reliably below the triple point of CH_4. Above 90 K, the root-mean-square deviations of the model predictions from the experimental data used in the fit ranged between 0.003 and 0.05 for x_{CH_4}, and between 0.01 and 0.03 for y_{CH_4}. Comparison with the experimental isopleths of Omar et al. (1962), the only experimental data below 90 K available at the time, yielded mixed results. For some isopleths the agreement was very good and taken as a validation of the model, while other isopleths showed notable offsets, the largest for $x_{CH_4} = 0.963$, which was also found suspect by Kouvaris and Flasar (1991). The non-systematic nature of the deviations was deemed a sign of substantial uncertainties in the data set from Omar et al. (1962).

Table 2
Clausius–Clapeyron (Eq. (14)) fits to experimental and calculated vapor pressure curves of pure N_2 (75 K $\leqslant T \leqslant$ 115 K) and pure CH_4 (95 K $\leqslant T \leqslant$ 135 K). Corresponding deviations from experimental data are shown in Fig. 1 (see Section 2.2 for the notation of potential models used in the MC simulations). Standard deviations of parameters are quoted in parentheses in terms of the least significant digit. d_{rms} is the root-mean-square deviation of the fit.

	A	B (K)	d_{rms}
CH_4			
Exp.	9.218 (31)	−1028.9 (35)	0.0087
L-CH_4	9.148 (43)	−1018.2 (48)	0.0118
S-CH_4	9.146 (44)	−1025.5 (50)	0.0123
F-CH_4	9.199 (26)	−1028.8 (29)	0.0063
C-CH_4	9.681 (66)	−903.9 (70)	0.0112
N_2			
Exp.	9.028 (12)	−697.46 (110)	0.0040
M1-N_2	8.989 (20)	−697.30 (180)	0.0066
M2-N_2	9.027 (10)	−697.40 (94)	0.0035
S-N_2	8.720 (13)	−646.71 (121)	0.0044
F-N_2	8.749 (11)	−672.17 (102)	0.0037

3. Results and discussion

3.1. Pure substances

In order to asses the quality of pure substance and cross-species interactions separately, we begin our analysis with a discussion of VLE curves of the pure substances. The equilibrium vapor pressures $P(T)$ of both substances follow a Clausius–Clapeyron form (Eq. (14)) almost perfectly with corresponding parameters listed in Table 2.

$$\ln(P/\mathrm{bar}) = A + B \cdot T^{-1} \tag{14}$$

For a LJ fluid the intercept A varies as $\ln\epsilon/\sigma^3$ and the slope B scales with ϵ. This allows for a simple analysis of the deviation of calculated curves from experimental data, which are shown in Fig. 1 together with the difference between the corresponding liquid densities $\rho(T)$.

Although derived in different ways, all three single site CH_4 potentials (L-CH_4, S-CH_4 , F-CH_4) have very similar LJ parameters, the largest differences being 2.15 K, and 0.0114 Å, respectively. These models yield accordingly similar results, which are in good agreement with the experimental data. By construction the L-CH_4 model reproduces the experiment near 140 K, but it increasingly overestimates the vapor pressure at lower temperatures (by 4% at 95 K). By contrast the S-CH_4 potential underestimates the vapor pressure by a roughly constant 4%, which indicates that the size parameter σ is slightly too high. Still the level of agreement is amazing for an *ab initio* potential – and presumably at least in part fortuitous. While these deviations are higher than the uncertainty in pressure measurements on Titan, <1% (Fulchignoni et al., 2005), they translate only into small errors $\Delta x_{CH_4} < 5 \times 10^{-3}$ based on our calculations. The best overall agreement is afforded by this work's F-CH_4 parameterization with pressures within 1% of experimental values, although at the expense of a slight overestimation of the liquid density by about 1.0%. Part of this remaining deviation is presumably a result of using the LJ EOS of Johnson et al. (1993) in our parameter refinement. Compared with the MC simulations, which are shown in Fig. 1, the EOS slightly overestimates the vapor pressure of the LJ fluid by about 1% above 105 K ($T^* = 0.7$), while liquid densities match almost perfectly. In the vicinity of the triple point of methane (90.68 K, $T^* \approx 0.6$), which lies outside the fitting range of the EOS, we observed a marked increase of the deviations between the EOS and our MC simulations to about 7% (or 8 mbar) in the vapor pressure. Here the EOS also overestimates the liquid density by about 1%. This already hints at limitations of the extrapolation of the LJ EOS significantly below the triple point of the LJ fluid $T^*_{triple} \approx 0.688$ (Agrawal and Kofke, 1995; Chen et al., 2001). At the same time it might indicate shortfalls of the single site LJ potential, which neglects the (presumably small) effects of the anisotropy of the $CH_4 \cdots CH_4$ interaction. Note that the single site LJ models all overestimate the triple point of CH_4 by more than 10 K, so that the experimental triple point lies already deep in the supercooled region of the LJ fluid.

The C-CH_4 model of Chao et al. (2009) performed rather poorly in reproducing the CH_4 VLE. Its liquid phase is far more volatile than the real liquid with a vapor pressure of 5 bar near the experimental boiling point. At the same time the liquid density between 95 K and 120 K exceeds experimental values by 7–10%. In this temperature range the predicted vapor pressure curve is still very well described by the Clausius–Clapeyron equation. The corresponding parameters in Table 2 indicate that both the well depth ϵ and the size parameter σ are significantly too small. Test calculations suggest that parameter values have to be increased by 10–20%, but without further systematic refinement we consider this potential model unsuitable for describing phase equilibria involving methane.

The M1-N_2 model was already validated by Carrero-Mantilla and Llano-Restrepo (2003). It provides a very good description of the VLE, even though liquid data were not included in the fit. The pressures and densities calculated with this model are systematically 4% too low and 1% too low, respectively, which indicates a size parameter σ that is slightly too large. Not surprisingly, the M2-N_2 model with the slightly decreased σ parameter brings the simulation results into virtually perfect agreement with experiment. With maximum deviations in the vapor pressure of about 4% our re-parameterized LJ-model, F-N_2, is comparable in average accuracy to the M1-N_2 model, but shows a systematic error in the slope of ln$P$ *vs* 1/T. While the vapor pressure might be brought into agreement with experiment (by reducing ϵ and σ^3 by the same factor), this would lead to serious errors in $\rho(T)$ and *vice versa*. Accordingly the S-N_2 parameterization with its significantly weaker interaction produces better agreement for liquid densities at the expense of larger errors in the vapor pressure. This inherent deficiency of the LJ potential model might arise from the neglect of anisotropy in the $N_2 \cdots N_2$ interaction, which appears to be correctly described by the M1 and M2 models. Even though this effect seems to be more important for N_2 than for CH_4, it is still only a minor contribution to the thermally averaged interaction in the liquid, as is apparent from the good description of the VLE curves by LJ fluids for both molecules almost down to the triple point.

Of the various potential models tested the results for pure substances would suggest the F-CH_4/M2-N_2 potential combination as the most promising model for the binary mixture.

3.2. The CH_4–N_2 binary system

We compared the performance of the models presented in Section 2 for the CH_4–N_2 system at five temperatures. The three lowest temperatures were chosen to span the different regimes in Titan's atmosphere. The temperature of 78.6 K corresponds to an altitude of 17.7 km, where the liquid phase of the system is assumed to be metastable (supercooled). Aerosol measurements determine a methane content of these droplets of 70 ± 7% (Wang et al., 2010a). At 81.6 K (13.2 km altitude) the liquid phase is in the stable range. The third temperature value (93.5 K) corresponds to the moon's surface where the presence of other substances might significantly shift the phase equilibrium. The last two values (112 and 130 K) correspond to the four lowest temperature/pressure data in the VLE measurements of Kidnay et al. (1975), which were used to determine the optimal scaling of the cross-interaction in the various potential models. The accuracy of the experimental values at 112 and 130 K is believed to be 1%.

Table 3
Comparing model VLE results with experimental data for the CH_4–N_2 mixture in terms of vapor ($Y = 100 \times y_{CH_4}$) and liquid ($X = 100 \times x_{CH_4}$) methane mole fractions.

T (K)	78.6		81.6		93.5		112		112		130		130	
P (bar)	0.568		0.734		1.466		1.965		4.332		4.155		6.594	
Composition	Y	X	Y	X	Y	X	Y	X	Y	X	Y	X	Y	X
Experiment[a]	2.34	70 ± 7	3.12		4.84		52.8	96.2	23.5	85.0	89.0	99.0	56.6	93.6
L-CH_4/M1-N_2[1.0][b]	2.01	53.3	2.75	56.9	9.26	73.0	52.6	93.9	21.6	77.5	89.0	98.5	54.6	90.3
F-CH_4/M2-N_2[1.0]	1.88	54.2	2.63	58.5	8.93	73.8	50.8	93.9	20.9	77.9	86.6	98.2	53.2	90.2
S-CH_4/S-N_2[1.0][c]	2.42	73.2	3.17	74.3	9.56	82.2	47.9	95.4	20.8	83.9	81.8	98.2	51.3	92.0
F-CH_4/F-N_2[1.0]	2.27	60.7	2.91	62.8	9.33	76.0	50.8	94.3	21.0	78.7	86.5	98.3	53.4	90.6
LJ–vdW1[1.0]	2.41	56.2	3.11	60.3	9.46	76.4	51.7	94.6	21.6	79.7	87.7	98.5	54.3	91.0
Thompson[d]	2.70	71.3	3.55	73.5	10.4	83.6	52.7	96.4	23.2	85.1				
Kouvaris[e]	2.71	71.6	3.55	73.3	10.3	82.8	53.0	96.2						
L-CH_4/M1-N_2[0.957][b]	2.79	70.9	3.65	74.0	10.7	84. 2	53.9	96.4	23.7	85.4	89.3	99.0	56.5	93.6
F-CH_4/M2-N_2[0.963]	**2.55**	**69.9**	**3.36**	**72.6**	**10.1**	**83.2**	**52.1**	**96.1**	**22.7**	**84.6**	**86.8**	**98.8**	**54.8**	**93.1**
S-CH_4/S-N_2[0.990][c]	2.54	76.5	3.33	77.7	9.77	84.2	50.3	95.8	22.0	84.8	84.4	98.5	53.2	92.7
F-CH_4/F-N_2[0.967]	2.83	74.9	3.64	76.6	10.2	84.1	51.9	96.2	22.7	84.8	87.0	98.8	54.8	93.1
LJ–vdW1[0.967]	3.06	66.2	3.82	70.5	10.5	84.3	52.6	96.4	23.1	85.7	88.1	98.9	55.6	93.5

[a] y_{CH_4} ($T \leqslant 94$ K) according to Niemann et al. (2005), x_{CH_4} (78.6 K) from Wang et al. (2010a), all other values from Kidnay et al. (1975).
[b] Potential of Carrero-Mantilla and Llano-Restrepo (2003).
[c] Potential of Shadman et al. (2009).
[d] EOS of Thompson et al. (1992). The EOS requires the vapor pressure of the pure components as input parameters and is thus limited to $T \leqslant T_{c,N_2} = 126.2$ K.
[e] EOS of Kouvaris and Flasar (1991).

Table 3 compares the results from molecular level MC simulations with those calculated with the three thermodynamic EOS presented in Section 2.3. The potential models are defined in terms of the pure substance potential functions of Section 2.2, and the scaling δ_ϵ of the cross-interaction between unlike molecules, which is given in brackets. The L-CH_4/M1-N_2[1.0] and S-CH_4/S-N_2[1.0] potential models have been used in Carrero-Mantilla and Llano-Restrepo (2003) and Shadman et al. (2009), respectively. In addition we tested our re-parameterized LJ potentials F-CH_4/F-N_2[δ_ϵ] and the F-CH_4/M2-N_2[δ_ϵ] combination, which was the most accurate for the pure substances. The statistical uncertainties of the MC results quoted in Table 3 only arise in the last digit given (with standard deviation of 1–2 units in the least significant digit, see Section 2.1).

For a given cross-interaction scaling δ_ϵ, the various potential models yield very similar compositions of the two phases above the triple point of methane, all within a few percent of each other. Predicted compositions are apparently fairly robust with respect to details of the pure substance potential functions. We note here the extremely good agreement between the LJ–vdW1 approximation and the corresponding explicit GCMC simulations (F-CH_4/F-N_2[δ_ϵ]). Deviations start to exceed the statistical uncertainties of the MC simulation significantly only below the triple point of methane. This is presumably not a pitfall of the van der Waals one-fluid theory, but simply due to the limited range of validity of the LJ EOS. The fit in Johnson et al. (1993) included data down to $T^* = 0.70$, while for a liquid mixture with $x_{CH_4} = 0.4$ a temperature of 80 K corresponds to $T^* = 0.67$ (from Eqs. (8) and (9)), which already lies in the supercooled region of the LJ fluid ($T^*_{triple} \approx 0.69$). That the error in composition is typically less than 10% still indicates a remarkable robustness of the parameterization given by Johnson et al. (1993) for extrapolation into the metastable region. Where applicable the other thermodynamic models of Thompson et al. (1992) and of Kouvaris and Flasar (1991) reproduce the experimental data within given error limits by construction. The only exception is the large deviation between the CH_4 content of 4.8% measured by Cassini-Huygens in the atmosphere near Titan's surface and the calculated values around 10% for the binary mixture. Since all models yield more or less the same value, this deviation presumably has its origin in the measured value as discussed below.

Without scaling the cross-interaction in the potentials (i.e. $\delta_\epsilon = 1.0$) the experimental data from Kidnay et al. (1975) lie clearly outside the scatter of the various potential models with relative deviations of up to 10%. This behavior suggests a common deficiency in describing the interaction of unlike molecules, although the effects of the individual potential parameters (ϵ_i, σ_i, δ_ϵ, δ_σ) are certainly not completely separable. To illustrate the sensitivity analysis of the potential models, Fig. 2 shows the parameter dependence of VLE compositions at $T = 93.5$ K and $P = 1.466$ bar predicted with the LJ–vdW1[δ_ϵ] EOS. σ_i and ϵ_i were changed over ±8%, δ_ϵ over ±10%. The dependence on the size parameter is relatively modest

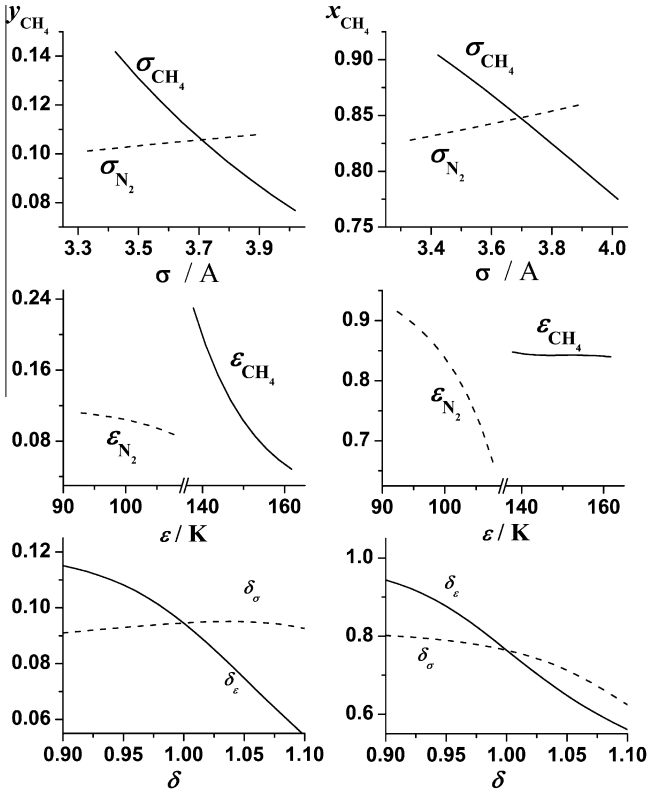

Fig. 2. Sensitivity analysis of compositions calculated with the LJ–vdW1 model for the vapor–liquid equilibrium of the CH_4–N_2 mixture at 93.5 K and 1.466 bar. The composition in terms of methane mole fractions in the vapor (y_{CH_4}) and in the liquid (x_{CH_4}) is shown as a function of σ_i (top), ϵ_i (center), δ_ϵ and δ_σ (bottom), i = CH_4, N_2.

with a more pronounced effect observed for changes in σ_{CH_4} than σ_{N_2}, as is to be expected for the larger species. Calculated compositions are about twice as sensitive to the interaction strength ϵ_i (in terms of relative parameter changes), where the vapor composition is mostly determined by ϵ_{CH_4}, while the liquid composition depends most strongly on ϵ_{N_2}. σ_i, and ϵ_i are determined within standard deviations of about 0.005 Å and 0.1 K, respectively, by fits to the vapor pressures and liquid densities of the pure substances. Within these limits the observed sensitivity of the composition does not allow for any significant improvement of the model potentials, which only leaves the cross-interaction scaling factors δ_σ and δ_ϵ as adjustable parameters. Given that the unscaled potentials tend to underestimate the CH_4 content of both phases, a reduction of δ_ϵ by a few percent should be able to significantly improve the agreement with experimental values. The calculated compositions are much less sensitive to δ_σ. The vapor phase composition is indeed virtually independent of δ_σ so that it could in principle be exploited for independent adjustments of the liquid composition alone. Since the effect would be rather small, and in order to keep the number of adjustable parameters at a minimum, we decided to leave $\delta_\sigma = 1.0$ for all further calculations.

Manually adjusting δ_ϵ to match the four reference data points from Kidnay et al. (1975) indeed drastically improves the overall agreement with experimental measurements and with the empirical thermodynamic models. The exception is the S-CH_4/S-N_2[δ_ϵ] potential. As discussed above, this model significantly overestimated the vapor pressure of liquid N_2 by about 30% in this temperature range (see Fig. 1). Thus it comes as no surprise that it systematically underestimates the methane content in the vapor of the binary mixture. With root-mean-square deviations (d_{rms}) in the methane mole fractions around 0.01 and maximum deviations (d_{max}) around 0.02, the F-CH_4/M2-N_2[δ_ϵ] model and our re-parameterized isotropic LJ potential, F-CH_4/F-N_2, yield comparable results. In this temperature and pressure range the anisotropy of the molecular interaction is apparently of only minor importance, which is clearly not the case at lower temperatures ($T < 100$ K). Here the isotropic potential systematically yields more methane-rich liquids (e.g. 75% vs. 71% at 78.6 K) because it cannot describe the increasing population of narrow deep wells that arise from the anisotropy of the N_2 interaction. Exhibiting only half the deviations from the experimental reference points ($d_{rms} = 0.005$, $d_{max} = 0.01$), the L-CH_4/M1-N_2[δ_ϵ] performs a little better than our re-parameterized version (F-CH_4/M2-N_2[δ_ϵ]), especially at higher (T,P), but such small variations lie doubtless within the uncertainty of the manual δ_ϵ-adjustment. The model that combines the best description of the pure substances, with the best agreement with experiment at 112 K and 1.965 bar (the reference point closest to the conditions prevalent on Titan) is obtained with the F-CH_4/M2-N_2[0.963] potential, which we thus consider to be the most reliable model (bold in Table 3). Comparing its predictions with results derived from the L-CH_4/M1-N_2[0.957] potential we estimate a relative uncertainty of about 5% for the calculated CH_4 partial pressure.

4. Conclusions

Our MC simulations yield predictions for the VLE of the CH_4–N_2 binary mixture in excellent agreement with available experimental data and extrapolate very well into the supercooled region of the phase diagram, which is relevant for Titan's atmosphere at altitudes above about 16 km. The comparison of different potential models and parameterizations show that the proper description of the densities in the phase equilibria of the pure substances is the key element in devising a reliable model for the mixture. With this, even simple Lorentz–Berthelot mixing rules yield reasonable predictions for the phase compositions in equilibrium. The extrapolation into the metastable region of supercooled liquids turned out to be more sensitive to the details of the cross-interaction of unlike molecules (see Table 3). We found that a simple scaling of the cross-interaction by a few percent brings all predicted compositions into close agreement with thermodynamic model equations of state, and with experiments where available. It is important to note that this small single-parameter adjustment can be derived from a single experimental data point in the stable region of the phase diagram. Our results show that the reference point need not even lie particularly close to the triple line, which means that the adjustment extrapolates in a remarkably stable fashion. Thus the optimal scaling for our re-parameterized LJ potential (F-CH_4/F-N_2) is $\delta_\epsilon = 0.967$, which is very close to the value of 0.958 obtained by Vrabec et al. (2009) at 140 K and 30 bar. The small reduction of the cross-interaction by a few percent, which we obtain for all model potentials, seems to reflect a general trend as similar adjustments have been found optimal for numerous other systems (McDonald, 1972; Vrabec et al., 2009). This demonstrates that even very simple pair potential models are capable of describing the VLE reliably and with the requisite accuracy for atmospheric modeling. Such model potentials keep the number of adjustable parameters at a minimum, which guarantees a reliable and stable extrapolation beyond the range of experimental reference data. For the present example we even reach the absolute minimum number of adjustable parameters, i.e. one parameter for each of the pure phases (essentially determined by known boiling points and liquid densities), and only a single parameter to describe the effect of mixing. The MC simulations can thus serve as a reference on a molecular level of theory to validate phenomenological EOS, which are more practical for atmospheric modeling. Note that the phenomenological EOS were derived and parameterized completely independently (Thompson et al., 1992; Kouvaris and Flasar, 1991).

By construction the thermodynamic models of Thompson et al. (1992) and Kouvaris and Flasar (1991) also agree very well with the experimental data on which their parameterization was based. At lower temperatures that lie outside the range of reliable experimental reference data these models slightly overestimate the CH_4 molar fraction in the vapor relative to the MC results. While the deviations appear to be systematic, they are comparable to the estimated uncertainty of the MC simulations and lie clearly within the experimental uncertainties quoted for the Cassini-Huygens data ($\Delta y_{CH_4} \sim 2 \times 10^{-3}$). Within this limit we can thus conclude that the MC simulations confirm and validate thermodynamic models commonly used in cloud models for Titan's atmosphere. Their validity even extends to supercooled liquids in the metastable region beyond the triple line of the mixture, which are relevant in Titan's atmosphere at altitudes above about 16 km. It is worth noting that the empirical EOS models of Thompson et al. (1992) and Kouvaris and Flasar (1991) yield virtually identical results over the whole range. The excellent agreement between the different calculated data is evidence for the internal consistency of the various approaches further supporting their reliability, in particular in view of the complete independence of the phenomenological thermodynamic models on the one hand, and the molecular level Monte Carlo simulations on the other.

Table 4 provides the aerosol phase compositions in Titan's atmosphere predicted as a function of altitude from our preferred potential model F-CH_4/M2-N_2[0.963]. The results are compared with predictions of the two thermodynamic models that were specifically designed for that purpose (Thompson et al., 1992; Kouvaris and Flasar, 1991), and with the gas phase compositions actually measured by the Huygens probe according to the analysis of Niemann et al. (2005). We expect MC predictions to be accurate to within a few percent (relative error) or 2–3 significant digits. All models predict an increase in the methane content of the droplets

Table 4
CH_4–N_2–aerosol phase composition in terms of vapor ($Y = 100 \times y_{CH_4}$) and liquid ($X = 100 \times x_{CH_4}$) methane mole fractions predicted for Titan's atmosphere as a function of altitude (h). Note that the droplets are supercooled above about 16 km (Omar et al., 1962) and solid above about 18.6 km (Wang et al., 2010a).

Cassini-Huygens[a]				Thompson[b]		Kouvaris[c]		This work[d]	
h (km)	T (K)	P (mbar)	Y_H	Y_c	X	Y_c	X	Y_c	X
18.592	78.0	540	1.96	2.54	70.6	2.56	70.8	2.43	69.0
17.717	78.6	568	2.34	2.70	71.3	2.71	71.4	2.54	69.8
17.041	79.0	591	2.42	2.80	71.5	2.81	71.5	2.69	70.5
16.227	79.5	619	2.68	2.96	72.0	2.96	72.0	2.83	70.8
15.546	80.0	644	2.65	3.07	72.2	3.06	72.0	2.89	70.6
15.250	80.2	654	2.65	3.12	72.4	3.11	72.1	3.00	71.8
14.159	81.0	696	2.73	3.38	73.2	3.37	73.0	3.16	71.4
12.538	82.1	762	3.23	3.73	74.0	3.71	73.7	3.54	73.0
11.805	82.5	793	3.49	3.84	74.1	3.81	73.6	3.63	72.7
11.084	83.1	825	3.51	4.09	74.8	4.05	74.4	3.90	73.9
10.479	83.5	853	3.35	4.24	75.1	4.20	74.7	4.05	74.4
9.932	84.0	878	3.77	4.44	75.6	4.39	75.2	4.17	74.2
9.089	84.6	919	3.90	4.64	75.8	4.60	75.4	4.43	75.0
8.508	85.0	948	4.12	4.85	76.3	4.80	75.9	4.58	75.2
7.810	85.6	985	4.47	5.09	76.7	5.03	76.2	4.85	75.8
7.524	85.8	1001	4.59	5.18	76.8	5.12	76.4	4.90	75.9
7.018	86.3	1027	4.80	5.47	77.4	5.40	77.1	5.20	76.5
5.050	88.1	1138	4.91	6.46	79.1	6.38	78.7	6.22	78.6
2.608	90.4	1289	4.84	7.89	80.9	7.80	80.3	7.57	80.3
0.310	93.1	1445	4.75	9.99	83.2	9.89	82.4	9.57	82.5
0.201	93.2	1453	4.69	10.11	83.3	10.00	82.5	9.63	82.5
0.068	93.4	1462	4.77	10.28	83.5	10.17	82.7	9.93	82.9

[a] Cassini-Huygens data according to Niemann et al. (2005).
[b] Thompson et al. (1992).
[c] Kouvaris and Flasar (1991).
[d] GEMC simulations with the F-CH_4/M2-N_2[0.963] potential model.

from 70% at high altitudes to over 80% at the surface. Our previous laboratory aerosol measurements found a methane content of 70 ± 7% for all altitudes above 13 km including the supercooled region above 16 km (Wang et al., 2010a), which is consistent with the results in Table 4. There exist no direct measurements of the composition of cloud droplets on Titan, neither from the Cassini-Huygens mission nor from any other observation. A comparison with the predicted values in Table 4 is thus not possible. However, the calculated gas phase equilibrium mole fractions of methane can be compared with the measured values from the Huygens probe (Niemann et al., 2005). Fig. 3 illustrates the deviations of the calculated equilibrium gas phase compositions from the measured Huygens values (Table 4). Since the methane gas phase mole fraction on Titan below about 7 km is much less than the equilibrium mole fraction, binary liquid methane–nitrogen clouds cannot be sustained at those altitudes as already discussed in earlier contributions (Tokano et al., 2006). Above 7 km, the calculations systematically predict slightly higher methane contents in the gas phase than determined by the Huygens probe (10–20% below according to EOS predictions, Fig. 3). The present study shows that such deviations lie outside the uncertainty of the predicted CH_4–N_2 VLE, so that the measured values from the Huygens probe (Niemann et al., 2005) appear to indicate undersaturation with respect to CH_4 condensation in the troposphere below 18.6 km altitude.

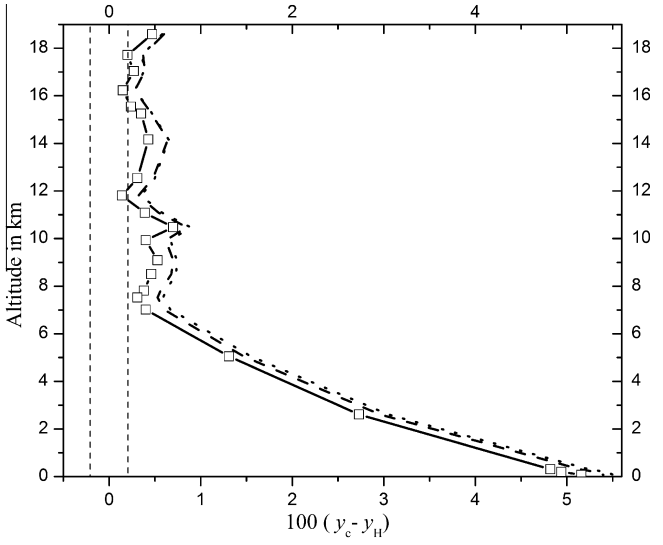

Fig. 3. Difference between calculated (y_c) and measured (y_H) methane gas phase mole fractions (see Table 4) as a function of the altitude. Full lines: MC simulations, this work. Dashed line: EOS of Kouvaris and Flasar (1991). Dotted line: EOS of Thompson et al. (1992). Measured data according to Niemann et al. (2005). The dashed vertical lines indicate the typical standard deviation of measurements.

A recent re-analysis of the Huygens data (Niemann et al., in press) puts methane mole fractions systematical about 10% above those quoted in Table 4. Table 5 compares the revised Huygens data with the corresponding predictions from the EOS models (Thompson et al., 1992; Kouvaris and Flasar, 1991) and from MC simulations with the F-CH_4/M_2–N_2[0.963] model potential. The deviations of the predicted VLE values from these revised data are shown in Fig. 4 with the typical standard deviation of measured methane mole fractions indicated by the vertical dashed lines. Within the uncertainty of the measurements, the revised methane partial pressures on Titan above 7 km now match the calculated equilibrium pressures exactly. The limit for supersaturation is thus completely determined by the experimental uncertainties yielding an upper limit of about 106% for those altitudes. We note that the neglect of N_2 dissolution (i.e. assuming an equilibrium with pure solid CH_4) would imply a saturation level of 90%. Note that the methane–nitrogen cloud droplets on Titan are expected to be large (Barth and Toon, 2006), so that the Kelvin effect on vapor pressures should be negligible. This result is consistent with the formation of binary methane–nitrogen clouds in this region on Titan and possibly speaks against important contributions from other molecular species such as ethane in these clouds near the Huygens landing

Table 5
CH_4–N_2–aerosol phase composition in Titan's atmosphere for the revised Cassini-Huygens data of Niemann et al. (in press). See Table 4 for definitions.

Cassini-Huygens[a]				Thompson[b]		Kouvaris[c]		This work[d]	
h (km)	T (K)	P (mbar)	Y_H	Y_c	X	Y_c	X	Y_c	X
18.3	78.5	563.2	2.60	2.69	71.31	2.70	71.48	2.46	68.96
16.6	79.6	620.9	2.83	2.98	72.14	2.98	72.07	2.79	70.57
15.3	80.4	665.8	3.02	3.20	72.68	3.19	72.46	3.03	71.61
13.8	81.4	724.9	3.36	3.50	73.33	3.47	72.95	3.35	72.74
11.3	83.2	827.4	3.97	4.14	75.00	4.11	74.67	3.94	74.25
9.5	84.4	909.4	4.39	4.57	75.63	4.52	75.19	4.30	74.52
8.3	85.4	969.9	4.99	5.01	76.57	4.95	76.18	4.75	75.67
6.7	86.8	1051.4	5.36	5.74	78.01	5.67	77.63	5.43	77.07
5.5	87.8	1118.4	5.55	6.25	78.75	6.17	78.32	5.93	77.86
4.5	88.8	1178.3	5.75	6.86	79.70	6.78	79.21	6.63	79.25
3.2	90.0	1257.2	5.76	7.61	80.63	7.52	80.05	7.37	80.26
2.0	91.2	1333.7	5.72	8.46	81.60	8.36	80.92	8.01	80.71
1.1	92.3	1393.8	5.73	9.37	82.64	9.27	81.90	8.94	81.88
0.3	93.1	1446.7	5.67	10.02	83.21	9.91	82.42	9.54	82.38

[a] Cassini-Huygens data according to Niemann et al. (in press).
[b] Thompson et al. (1992).
[c] Kouvaris and Flasar (1991).
[d] GEMC simulations with the F-CH_4/M2-N_2[0.963] potential model.

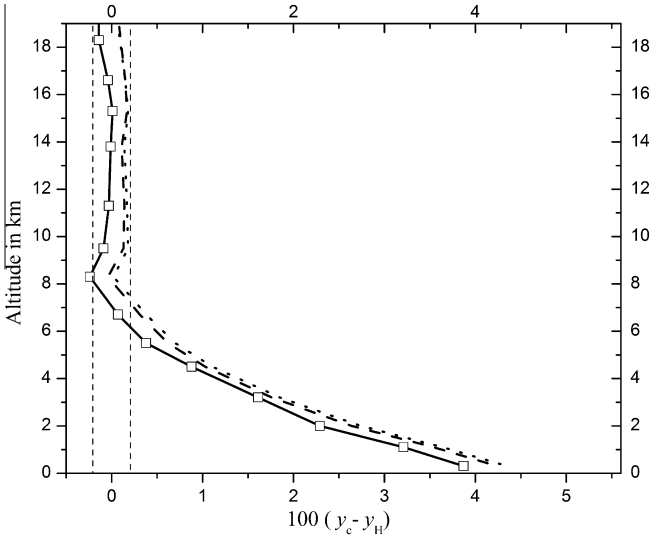

Fig. 4. Difference between calculated (y_c) and measured (y_H) methane gas phase mole fractions (see Table 5) as a function of the altitude. Full lines: MC simulations, this work. Dashed line: EOS of Kouvaris and Flasar (1991). Dotted line: EOS of Thompson et al. (1992). Measured data according to Niemann et al. (in press). The dashed vertical lines indicate the typical standard deviation of measurements.

site. Furthermore, the fact that the methane vapor pressure above 16 km is the same as that over the supercooled liquid, together with our previous observation that supercooled liquid droplets can be sustained under these conditions in the laboratory, might be an indication that a supercooled cloud layer indeed exists on Titan.

The successful validation of MC models using simple pair potentials to predict the binary aerosol phase composition under conditions found in Titan's atmosphere holds promise for the extension to ternary or even more complex mixtures. With the viability of the approach in principle established by the present study it should be possible to investigate the fate of ethane in Titan's atmosphere, which is assumed to be a major constituent of polar ethane clouds and of lakes on the moon's surface (Griffith et al., 2006; Cordier et al., 2009). Contrary to current assumptions, recent aerosol experiments from our laboratory show that especially in mixtures with methane and possibly nitrogen, ethane could very well stay liquid throughout most of the atmosphere (Wang et al., 2010b; Lang, E.K., Knox, K.J., Wang, C.C., Signorell, R., 2010, submitted for publication). Due to the lack of experimental data at low temperatures, phenomenological thermodynamic models are less reliable to predict the phase equilibrium of mixtures containing ethane. Based on the promising results for the binary methane–nitrogen system we are currently developing molecular models for Monte Carlo simulations to fill this gap.

Acknowledgments

We acknowledge support from the Natural Sciences and Engineering Research Council of Canada, from the Canada Foundation for Innovation, and from the Cassini-Huygens mission. This research has been enabled through the generous allocation of advanced computing resources by WestGrid and Compute/Calcul Canada.

References

Ádámkovics, M., Barnes, J.W., Hartung, M., de Pater, I., 2007. Widespread morning drizzle on Titan. Science 318, 962–965.
Agrawal, R., Kofke, D.A., 1995. Thermodynamic and structural-properties of model systems at solid–fluid coexistence. 2. Melting and sublimation of the Lennard–Jones system. Mol. Phys. 85, 43–59.
Allen, M.P., Tildesley, D.J., 1988. Computer Simulations of Liquids. Oxford University Press, New York.
Angus, S., Armstrong, B., de Reuck, K.M., 1978. International thermodynamic tables of the fluid state. 5. Methane. International Union of Pure and Applied Chemistry, Chemical Data Series No. 16, Pergamon Press, Oxford.
Angus, S., Armstrong, B., de Reuck, K.M., 1979. International thermodynamic tables of the fluid state. 6. Nitrogen. International Union of Pure and Applied Chemistry, Chemical Data Series No. 20, Pergamon Press, Oxford.
Atreya, S.K., Adams, E.Y., Niemann, H.B., Demick-Montelara, J.E., Owen, T.C., Fulchignoni, M., Ferri, F., Wilson, E.H., 2006. Titan's methane cycle. Planet. Space Sci. 54, 1177–1187.
Barth, E.L., Rafkin, S.C.R., 2007. TRAMS: A new dynamic cloud model for Titan's methane clouds. Geophys. Res. Lett. 34, L03203.
Barth, E.L., Rafkin, S.C.R., 2010. Convective cloud heights as a diagnostic for methane environment on Titan. Icarus 206, 467–484.
Barth, E.L., Toon, O.B., 2006. Methane, ethane, and mixed clouds in Titan's atmosphere: Properties derived from microphysical modeling. Icarus 182, 230–250.
Bender, E., 1975. Calculation of phase equilibria and thermodynamic properties of cryogenic mixtures with a new equation of state. In: Proceedings, International Congress on Chemical Engineering. Chem. Equip. Des. Autom. F, f2.13–f2.28.
Carrero-Mantilla, J., Llano-Restrepo, M., 2003. Vapor–liquid equilibria of the binary mixtures nitrogen plus methane, nitrogen plus ethane and nitrogen plus carbon dioxide, and the ternary mixture nitrogen plus methane plus ethane from Gibbs-ensemble molecular simulation. Fluid Phase Equilib. 208, 155–169.

Chao, S.W., Li, A.H.T., Chao, S.D., 2009. Molecular dynamics simulations of fluid methane properties using ab initio intermolecular interaction potentials. J. Comput. Chem. 30, 1839–1849.
Chen, B., Potoff, J.J., Siepmann, J.I., 2001. Monte Carlo calculations for alcohols and their mixtures with alkanes. Transferable potentials for phase equilibria. 5. United-atom description of primary, secondary, and tertiary alcohols. J. Phys. Chem. B 105, 3093–3104.
Cheung, H., Wang, D.I.J., 1964. Solubility of volatile gases in hydrocarbon solvents at cryogenic temperatures. Ind. Eng. Chem. Fundam. 3, 355–361.
Cines, M.R., Roach, J.T., Hogan, R.J., Roland, C.H., 1953. Nitrogen-methane vapor–liquid equilibria. Chem. Eng. Prog. Symp. Ser. No. 6 49, 1–10.
Cordier, D., Mousis, O., Lunine, J.I., Lavvas, P., Vuitton, V., 2009. An estimate of the chemical composition of Titan's lakes. Astrophys. J. Lett. 707, L128–L131.
De Kok, R., Irwin, P.G.J., Teanby, N.A., 2010. Far-infrared opacity sources in Titan's troposphere reconsidered. Icarus 209, 854–857.
Frenkel, D., Smit, B., 2001. Understanding Molecular Simulation: From Algorithms to Applications, second ed. Academic Press.
Fulchignoni, M. et al., 2005. In situ measurements of the physical characteristics of Titan's environment. Nature 438, 785–791.
Graves, S.D.B., McKay, C.P., Griffith, C.A., Ferri, F., Fulchignoni, M., 2008. Rain and hail can reach the surface of Titan. Planet. Space Sci. 56, 346–357.
Griffith, C.A. et al., 2006. Evidence for a polar ethane cloud on Titan. Science 313, 1620–1622.
Hayden, J.G., O'Connell, J.P., 1975. A generalized method for predicting second virial coefficients. Ind. Eng. Chem. Process Des. Dev. 14, 209–216.
Iglesias-Silva, G.A., Holste, J.C., Eubank, P.T., Marsh, K.N., Hall, K.R., 1987. A vapor pressure equation from extended asymptotic behaviour. AIChE J. 33, 1550–1556.
Johnson, J.K., Zollweg, J.A., Gubbins, K.E., 1993. The Lennard–Jones equation of state revisited. Mol. Phys. 78, 591–618.
Kidnay, A.J., Miller, R.C., Parrish, W.R., Hiza, M.J., 1975. Liquid–vapour phase equilibria in the N_2–CH_4 system from 130 to 180 K. Cryogenics 15, 531–540.
Kim, S.J., Trafton, L.M., Geballe, T.R., 2008. No evidence of morning or large-scale drizzle on Titan. Astrophys. J. Lett. 679, L53–L56.
Kouvaris, L.C., Flasar, F.M., 1991. Phase equilibrium of methane and nitrogen at low temperatures: Application to Titan. Icarus 91, 112–124.
Lemmon, E.W., McLinden, M.O., Friend, D.G., 2010. Thermophysical properties of fluid systems. In: Linstrom, P.J., Mallard, W.G. (Eds.), NIST Chemistry WebBook, NIST Standard Reference Database Number 69. National Institute of Standards and Technology, Gaithersburg, MD (retrieved 14.10.10). <http://webbook.nist.gov>.
Lotfi, A., 1993. Dr.-Ing. thesis at Ruhr-Universität, Bochum. See also Fortschr. Ber. VDI, Reihe 3, Nr. 335, VDI-Verlag, Düsseldorf.
Lunine, J.I., Atreya, S.K., 2008. The methane cycle on Titan. Nat. Geosci. 1, 159–164.
Martin, M.G., Siepmann, J.I., 1997. Predicting multicomponent phase equilibria and free energies of transfer for alkanes by molecular simulation. J. Am. Chem. Soc. 119, 8921–8924.
McClure, D.W., Lewis, K.L., Miller, R.C., Staveley, L.A.K., 1976. Excess enthalpies and Gibbs free energies for nitrogen + methane at temperatures below the critical point of nitrogen. J. Chem. Thermodyn. 8, 785–792.
McDonald, I.R., 1972. NpT-ensemble Monte Carlo calculations for binary liquid mixtures. Mol. Phys. 23, 41–58.
McDonald, I.R., 1973. Statistical Mechanics, vol. 1 (edited by K. Singer, Specialist Periodical Report, The Chemical Society, London).
Murthy, C.S., Singer, K., Klein, M.L., McDonald, I.R., 1980. Pairwise additive effective potentials for nitrogen. Mol. Phys. 41, 1387–1399.
Niemann, H.B., Atreya, S.K., Demik, J.E., Gautier, D., Haberman, J.A., Harpold, D.N., Kasprzak, W.T., Lunine, J.I., 2010. The composition of Titan's lower atmosphere and simple surface volatiles as measured by the Cassini-Huygens probe gas chromatograph mass spectrometer experiment. J. Geophys. Res. 115, E12006, doi:10.1029/2010JE003659.
Niemann, H.B. et al., 2005. The abundances of constituents of Titan's atmosphere from the GCMS instrument on the Huygens probe. Nature 438, 779–784.
Omar, M.H., Dokoupil, Z., Schroten, H.G.M., 1962. Determination of the solid–liquid equilibrium diagram for the nitrogen–methane system. Physica 28, 309–329.
Orbey, H., Vera, J.H., 1983. Correlation of the third virial coefficient using P_c, T_c and ω as parameters. AIChE J. 29, 107–113.
Panagiotopoulos, A.Z., 1989. Exact calculations of fluid-phase equilibria by monte carle simulation in a new statistical ensemble. Int. J. Thermophys. 10, 447–457.
Parrish, W.R., Hiza, M.J., 1974. Liquid–vapor equilibria in the nitrogen–methane system between 95 and 120 K. Adv. Cryog. Eng. 19, 300–308.
Penteado, P.F., Griffith, C.A., Tomasko, M.G., Engel, S., See, C., Doose, L., Baines, K.H., et al., 2010. Latitudinal variations in Titan's methane and haze from Cassini VIMS observations. Icarus 206, 352–365.
Potoff, J.J., Siepmann, J.I., 2001. Vapor liquid equilibria of mixtures containing alkanes, carbon dioxide, and nitrogen. AIChE J. 47, 1676–1682.
Prausnitz, J.M., 1969. Molecular Thermodynamics of Fluid-Phase Equilibria. Prentice-Hall, Englewood Cliffs, NJ.
Schindler, H., Vogelsang, R., Staemmler, V., Siddiqi, M.A., Svejda, P., 1993. Ab initio intermolecular potentials of methane, nitrogen and methane + nitrogen and their use in Monte Carlo simulations of fluids and fluid mixtures. Mol. Phys. 80, 1413–1429.
Setzmann, U., Wagner, W., 1991. A new equation of state and tables of thermodynamic properties for methane covering the range from the melting line to 625 K at pressures up to 1000 MPa. J. Phys. Chem. Ref. Data 20, 1061–1155.
Shadman, M., Yeganegi, S., Ziaie, F., 2009. Ab initio interaction potential of methane and nitrogen. Chem. Phys. Lett. 467, 237–242.
Sprow, F.B., Prausnitz, J.M., 1966. Vapor–liquid equilibria for five cryogenic mixtures. AIChE J. 12, 780–784.
Stryjek, R., Chappelear, P.S., Kobayashi, R., 1974. Low-temperature vapor–liquid equilibria of nitrogen–methane system. J. Chem. Eng. Data 19, 334–339.
Szczesniak, M.M., Chalasinski, G., Cybulski, S.M., Scheiner, S., 1990. Intermolecular potential of the methane dimer and trimer. J. Chem. Phys. 93, 4243–4253.
Thompson, W.R., Zollweg, J.A., Gabis, D.H., 1992. Vapor–liquid equilibrium thermodynamics of N_2 + CH_4: Model and Titan applications. Icarus 97, 187–199.
Tokano, T., McKay, C.P., Neubauer, F.M., Atreya, S.K., Ferri, F., Fulchignoni, M., Niemann, H.B., 2006. Methane drizzle on Titan. Nature 442, 432–435.
Tomasko, M.G. et al., 2005. Rain, winds and haze during the Huygens probe's descent to Titan's surface. Nature 438, 765–778.
Valleau, J.P., 1998. Number-dependence concerns in Gibbs-ensemble Monte Carlo. J. Chem. Phys. 108, 2962–2966.
Vrabec, J., Fischer, J., 1996. Vapor–liquid equilibria of binary mixtures containing methane, ethane, and carbon dioxide from molecular simulation. Int. J. Thermophys. 17, 889–908.
Vrabec, J., Huang, Y.-l., Hasse, H., 2009. Molecular models for 267 binary mixtures validated by vapor–liquid equilibria: A systematic approach. Fluid Phase Equilib. 279, 120–135.
Vrabec, J., Stoll, J., Hasse, H., 2001. A set of molecular models for symmetric quadrupolar fluids. J. Phys. Chem. B 105, 12126–12133.
Wang, C.C., Atreya, S.K., Signorell, R., 2010a. Evidence for layered methane clouds in Titan's troposphere. Icarus 206, 787–790.
Wang, C.C., Lang, E.K., Signorell, R., 2010b. Methane gas stabilizes supercooled ethane droplets in Titan's clouds. Astrophys. J. Lett. 712, L40–L43.